P 2231

Joint Institute for Nuclear Research, Dubna

Report No. P 2231

An Estimation of Ionizing Radiation Levels near the 10 GeV Synchrophasotron of the Joint Institute for Nuclear Research

by

M.M. Komochkov and V.N. Lebedev

Translated at CERN by A.T. Sanders
and revised by N. Mouravieff
(Original : Russian)

(CERN Trans. 66-1)

Geneva
January, 1966

66/59/5
p/eht

At the present time there is still no sufficiently well-founded method of calculating the radiation field near proton accelerators with an energy of over 1 GeV. There are two reasons for this. The first is the lack of the necessary experimental data. The second is the fact that radiation levels are affected by a large number of factors, which it is either difficult or impossible to take into account in calculations. Consequently, estimation of the thickness of the shielding for new high-energy accelerators being constructed is particularly rough and is made on the basis of assumptions which have not been proved in practice; this eventually leads to unsound use of resources, whether the thickness of the shielding is over- or underestimated, in which case it is subsequently necessary to create additional shielding. Under these circumstances any additional information is useful. In this paper an attempt is made to calculate the dose due to the basic components of the radiation, on the basis of a very simple model of the propagation of radiation near the 10 GeV synchrophasotron, taking into account the basic elements of its construction.

1. CONSTRUCTIONAL CHARACTERISTICS OF THE SYNCHROPHASOTRON AND ITS SHIELDING

The synchrophasotron is a proton synchrotron with weak focusing. The maximum energy of the accelerated protons is 10 GeV. The protons are first accelerated in a linear accelerator up to 9 MeV and are then introduced into the synchrophasotron vacuum chamber. The vacuum chamber has an aperture of 2×0.30 m^2 and an over-all length of 208 m. The chamber walls are double: the inner walls are made of stainless steel 5 mm thick, and the outer of dural. The chamber is situated between the poles of a ring-shaped magnet consisting of four quadrants. The quadrants are separated by straight gaps 8 metres long and consist of 48 paired sections, as shown in the diagram, each section having windows on both sides to take the servo of the pneumatic targets, the vacuum pump lines, etc. The width of the magnet yoke is 1.67 m on the inner side of the ring and 1.48 m on the outer side. The reader will find more details of characteristics and a description of the synchrophasotron in another paper[1].

When planning the synchrophasotron it was supposed that the magnet yoke would function as the basic shielding. According to this principle, and in view of the fact that the rated current of the proton beam was to be 10^8-10^9 protons/sec^{-1}, the basic walls of the accelerator building were made of brick 0.6 m thick and with a large amount of window openings. For physics apparatus and staff there are two halls (18 and 20 in Fig. 1). One of them (18) is separated from the main hall by a monolithic wall of ordinary concrete 8 m thick. The second hall (20) is separated by two concrete walls of an over-all thickness of about 4 m in the plane of the proton beam orbit. Laboratory space is provided in the basement in a hall 1-2 m below the orbit plane, and the upper ceiling of this area is made of monolithic concrete of a thickness of 1 m. A more detailed description of the construction of the shielding walls and the building as a whole is to be found in another paper[2].

At present, the synchrophasotron operates at an intensity of the internal beam of over 1×10^{11} protons/cycle^{-1} and a repetition rate of 6.6 cycle/min.

2. BASIC PREREQUISITES FOR CALCULATING THE RADIATION LEVELS NEAR THE SYNCHROPHASOTRON

The basic radiation sources are the walls of the vacuum chamber, which the protons that have left the accelerated beam penetrate, and the targets inside the synchrophasotron chamber. Radiation from the sources passes mainly through three parts of the accelerator: the straight sections, the "windows" in the magnet yoke and the gaps between the sections of the magnet quadrant, and also the magnet yoke itself.

The basic expression for calculating the density of the high-energy neutron flux Φ^h ($E_I \geq 20$ MeV) at a certain point A, from all possible targets, including the walls of the accelerator chamber, will be

$$\Phi^b = f \sum_j \frac{i_j g_j(\vartheta)}{r_j^2} e^{-\frac{x_j}{\lambda}} \qquad (1)$$

66/59/5
p/eht

Here i_j is the accelerated protons flux per pulse falling on the j^{th} target;

f is the pulse rate;

$g_j(\vartheta)$ is the flux of neutrons of over 20 MeV at an angle ϑ to the proton beam in a solid angle of 1 steradian for one proton from the j^{th} target;

r_j is the distance from the target to point A;

x_j is the thickness of the shielding in the direction $\vec{r}_j$;

λ is the attenuation length of the flux of neutrons of over 20 MeV.

The density of the flux Φ^f of fast neutrons of 0.1 - 20 MeV emerging from the target, the thickness of which is equal to the length of the inelastic interaction of protons and nuclei, will be determined by means of the equation:

$$\Phi = \frac{f.i.k}{4\pi r^2}, \qquad (2)$$

where k is the average number of fast neutrons produced in one inelastic collision of protons and the nuclei of the elements making up the target. In accordance with the data given in another paper[3], the value "k" will be chosen as ~ 10 for copper and iron. When establishing equation (2) it was considered that the reduction in the output of fast neutrons owing to the attenuation of the primary proton current in the target was offset by the production of fast neutrons by high-energy secondary particles[4].

The calculations will be made on the following assumptions:

1. The flux of protons scattered by the target or extracted from the beam as a result of losses upon acceleration or scattering on gas, or for other reasons, steadily penetrates the walls of the accelerator vacuum chamber. With a thin internal target almost all the accelerated proton flux is scattered in the vacuum chamber. In this case $i_j = (I/L)\Delta L_j$, where I is the total proton flux in a pulse, and L is the length of the vacuum chamber.

66/59/5
p/eht

2. Let us take the thickness of all the targets, including also the effective thickness of the chamber walls in the direction of motion of the protons falling on the wall, as equal to the length of the inelastic interaction of protons and nuclei (~ 100 g/cm^2). This is near to the actual conditions and allows the use of the data concerning the values of $g(\vartheta)$, estimated by Moyer[3] for proton energies of 6.3 GeV.

3. The output of cascade neutrons from a target hit by 10 GeV protons $g(\vartheta)$, according to Moyer[3] and Geibel and Ranft[5] may be determined be means of the following relation:

$$g_{10}(\vartheta) \cong 1.5\, g_{6,3}(\vartheta)\ , \qquad (3)$$

where $g_{6,3}(\vartheta)$ is the flux of neutrons with an energy of over 150 MeV upon interaction with a 6.3 GeV proton target, and $g_{10}(\vartheta)$ is the flux of neutrons of over 20 MeV upon interaction between the target and a 10 GeV proton.

4. The attenuation length of the neutron flux from the target does not depend on the angle ϑ and for neutrons of over 20 MeV is: for ordinary concrete (ρ = 2350 kg/m^{-3}) - 1430 kg/m^{-2} [6]; for heavy concrete (ρ = 3850 kg/m^{-3}) - 1800 kg/m^{-2} [7]; for iron - 1800 kg/m^{-2} [6,7].

5. The ratio between the flux of fast neutrons of 0.1 - 20 MeV and the flux of neutrons of over 20 MeV beyond the shielding is found by means of the following relation:

$$\frac{\Phi^f}{\varphi^h} = \frac{\sigma_{ii}\, k_3}{\sigma^f_{extr} - \sigma^h_{extr}}\ . \qquad (4)$$

Here σ_{ii} is the inelastic interaction cross-section of high-energy neutrons (> 100 MeV) [in a report[8] it is shown that σ_{ii} satisfies the empirical relation: $\sigma_{ii} = 32\, A^{3/4} \times 10^{-31} M^2$], σ^f_{extr} and σ^h_{extr} are the cross-sections of the extraction of fast neutrons and high-energy neutrons, respectively; k_3 is the average number of fast neutrons produced in one inelastic collision of high-energy neutrons and the nuclei of the elements making up the shielding. Data on the values of k_3 are also given in the

report[8]). Expression (4) can easily be obtained from the condition of the exponential law of neutron attenuation in shielding. For light materials (for instance, ordinary concrete) the value Φ^f/Φ^h is approximately 0.4, and for medium elements (for instance, iron) this ratio is ≈ 0.7. For estimating the values of k_3 the mean energy of high-energy neutrons was assumed to be a few hundred MeV.

6. The 1-1.5 MeV neutron flux Φ_n, emerging from the heavy concrete shielding is approximately three times the high-energy neutron flux with $E > 20$, passing through the shielding. The Φ_n neutron flux emerging from iron shielding may be almost 400 times the high-energy neutron flux. This occurs as a result of the storage of neutrons of intermediate energy, the attenuation length of whose current in iron is greater than the attenuation length of the high-energy neutron flux. For neutrons of intermediate energy emerging from the shielding in the opposite direction to the high-energy neutron beam, the relation $\Phi^n/\Phi^h \cong 0.6$ is approximately correct for concrete, and $\Phi^n/\Phi^h \cong 3.8$ for iron. The spectrum of the intermediate neutrons emerging from the shielding may be approximately described by the expression $1/E$. These data were obtained by solving the transfer equation in the age-diffusion approximation.

7. The radiation dose due to a known neutron flux was calculated (taking into account the supposed spectrum) in terms of the following doses for a single current of neutrons of different energy:

0.1	microrem.neutr.$^{-1}$	cm^2	(E > 20 MeV),
0.041	microrem.neutr.$^{-1}$	cm^2	(20 MeV > E > 0.1 MeV),
0.0053	microrem.neutr.$^{-1}$	cm^2	(1.5 MeV > E > 1 eV),
0.0018	microrem.neutr.$^{-1}$	cm^2	(0.1 MeV > E > 1 eV).

The validity of the values assumed is discussed in Ref. 5). The values given practically coincide with those recommended in Ref. (9).

8. The dose of gamma-radiation is 15% of the dose due to neutrons of over 0.1 MeV.

66/59/5
p/cht

9. The contribution of mesons and thermal neutrons to the total biological dose is negligible.

The flux density of fast neutrons at great distances from the synchrophasotron was calculated by the method proposed by Lindenbaum[7], and by means of the following empirical equation, proposed by Thomas[10]:

$$\Phi^f = \frac{Q}{4\pi r^2} a[1 - \exp(-r/\lambda_1)]\exp(-r/\lambda_2) \qquad (5)$$

where λ_1 = 58 m; λ_2 = 267 m; a = 2.8; Q is the total flux of neutrons of over 0.1 MeV emerging beyond the yoke of the synchrophasotron; r is the distance from the centre of the accelerator hall to the point concerned.

3. RESULTS OF THE CALCULATION. COMPARISON WITH THE EXPERIMENT

The results of the calculation of the radiation level near the synchrophasotron are given in Table 1, which also gives the experimental data for purposes of comparison. The numbers of the points to which the calculations and measurements refer are marked on the diagram. The high-energy neutrons and protons were recorded by the radioactivity induced in carbon ($E_I \geqq 20$ MeV); the fast, intermediate and thermal neutrons were recorded by means of a BF_3 counter in paraffin moderator screens of different thicknesses, the gamma-radiation by means of free-air ionization chambers and X-ray films. All the experimental data are taken from papers[5,11]. The calculated and measured values of the radiation level are normalized to a proton flux of 10^{10} with target 21 placed inside the quadrant before the straight section marked 6 in the diagram. Comparison of the calculated and the measured level shows that although for the total dose the data appear to agree well, nevertheless, for the separate components of the radiation the difference between the experimental and the calculated value may be considerable (a factor 2-2.5). This difference is due to the extremely complex space distribution of the sources and absorbers, which it is very difficult to take into account in the calculations.

66/59/5
p/eht

Table 2 gives a comparison of the calculated and measured values of the neutron flux at relatively great distances from the centre of the synchrophasotron. The total neutron flux of over 1.5 MeV - Q [see Eq. (2)] comprises the neutron flux from the straight sections, equal to 2.8×10^{10} neutrons $\times 10^{-10}$ protons, and the neutron flux emerging from the windows in the magnet yoke, which is equal to 0.18×10^{10} neutrons $\times 10^{-10}$ protons. A comparison of the data of Table 2 shows that the empirical equation (2) does not express the dependence of the neutron flux on the distance as well as does the equation developed by Lindenbaum[7]. The considerable difference in the absolute values of the neutron fluxes given in Ref. 11) and those obtained by calculation is due to the fact that on the one hand the contribution is the flux of neutrons with an energy of less than 0.1 MeV, and on the other hand the attenuation of the flux in the walls of the building were not taken into account.

66/59/5
p/eht

P/66/44

TABLE 1

Radiation levels near the 10 GeV Synchrophasotron

No. of points in Fig. 1	Density of particle flux, part/cm^{2}10^{10} protons						Gamma radiation dose microrem/10^{10} protons		Total dose microrem/10^{10} protons	
	Nucleons E > 20 MeV	Neutrons E > 20 MeV	Fast neutrons 20 MeV ≥ E ≥ 0.1 MeV		Intermediate neutrons 0.1 MeV ≥ E ≥ 1 eV	1.5 MeV ≥ E ≥ 1 eV				
	Measured	Calculated	Measured	Calculated	Measured	Calculated	Measured	Calculated	Measured	Calculated
22	1640	1300	-	1900	-	5000	-	31	220	264
23	700	630	520	700	960	2400	3,4	13,6	94	118
24	130	120	550	210	630	450	4,9	3,1	30	26
25	140	120	290	210	840	450	3,8	3,1	24	26
26	170	120	260	210	520	450	2,6	3,1	24	26
27	160	120	205	210	380	450	3,4	3,1	27	26
28	100	120	260	210	760	450	3	3,1	21	26
29	1150	670	1650	1500	2300	2550	26	19,0	185	160
30	700	670	2150	1500	3250	2550	23	19,0	155	160
31	85	90	400	340	730	340	2,4	3,4	19,2	28
32	950	900	750	480	1120	3400	20	16,4	130	144
33	20	20	9	6[x]	23	60	-	0,3	2,6	2,9
34	140	150	150	160	250	570	I	3,2	20	28
35	30	55[xx]	16	50[xx]	32	210[xx]	-	1,1	3,7	9,7
36	-	18	3,5	6[x]	9	-	-	0,3	1,4	2,3
37	42	35	58	-	122	130	0,5	~ I	7	8,7
38	12	16	II	-	25	60	0,5	~ 0,5	1,7	4,3
39	364	300	-	820	-	1100	-	9,5	~ 76	79
40	127	60	-	160	-	230	-	1,9	~ 26	15,5

x) The attenuation of the fast neutron flux in the brick wall was taken into account when making the calculation (λ_f = 24 cm).

xx) The attenuation of the neutron flux in the magnet lenses was not taken into account when making the calculation.

TABLE 2

Density of neutron flux at great distances from the synchrophasotron

Distance from the geometrical centre of the synchrophasotron hall, metres		123	185	255	314	384	485
Density of fast and intermediate neutron flux ($1\ eV < E < 20\ MeV$) neutrons/ $cm^2 10^{10}$ protons	Experimental data[1,2]	14,2	7,5	2,82	1,84	1,28	0,82
	Calculated according to Eq. (5)	24,0	8,70	4,15	2,10	1,13	0,52
	Calculated by Lindenbaum's method[7]	27,0	13,0	7,45	4,40	2,75	1,52
Comparison of results	Φ_2 / Φ_1	1,7	1,2	1,5	0,9	0,9	0.6
	Φ_3 / Φ_1	1,90	1,73	2,6	2,4	2,2	1,85

66/59/5
p/eht

Figure Caption

Fig. 1 : Plan of synchrophasotron building and layout of local shielding (thickness of the black sections is proportional to the thickness of the shielding).

1. 570 keV pre-injector hall.
2. 9 MeV linac.
3. Linac control desk.
4. Straight accelerating sections.
5. Input straight section.
6. Output straight section.
7. Positive K-meson channel.
8. Intermediate K-meson channel.
9. Negative K-meson channels.
10. Neutral particle channels.
11. Concrete blockhouse.
12. Slow K-meson channel.
13. Auxiliary control desk,
14. Positive K-meson channel.
15. Neutral K-meson channel.
16. Positive π-meson channel.
17. Laboratories in basement.
18. Physics barrack.
19. Auxiliary rooms.
20. Physics barrack.
21. Operating targets on which measurements were made.

22-40. Points of measurement.

66/59/5
p/eht

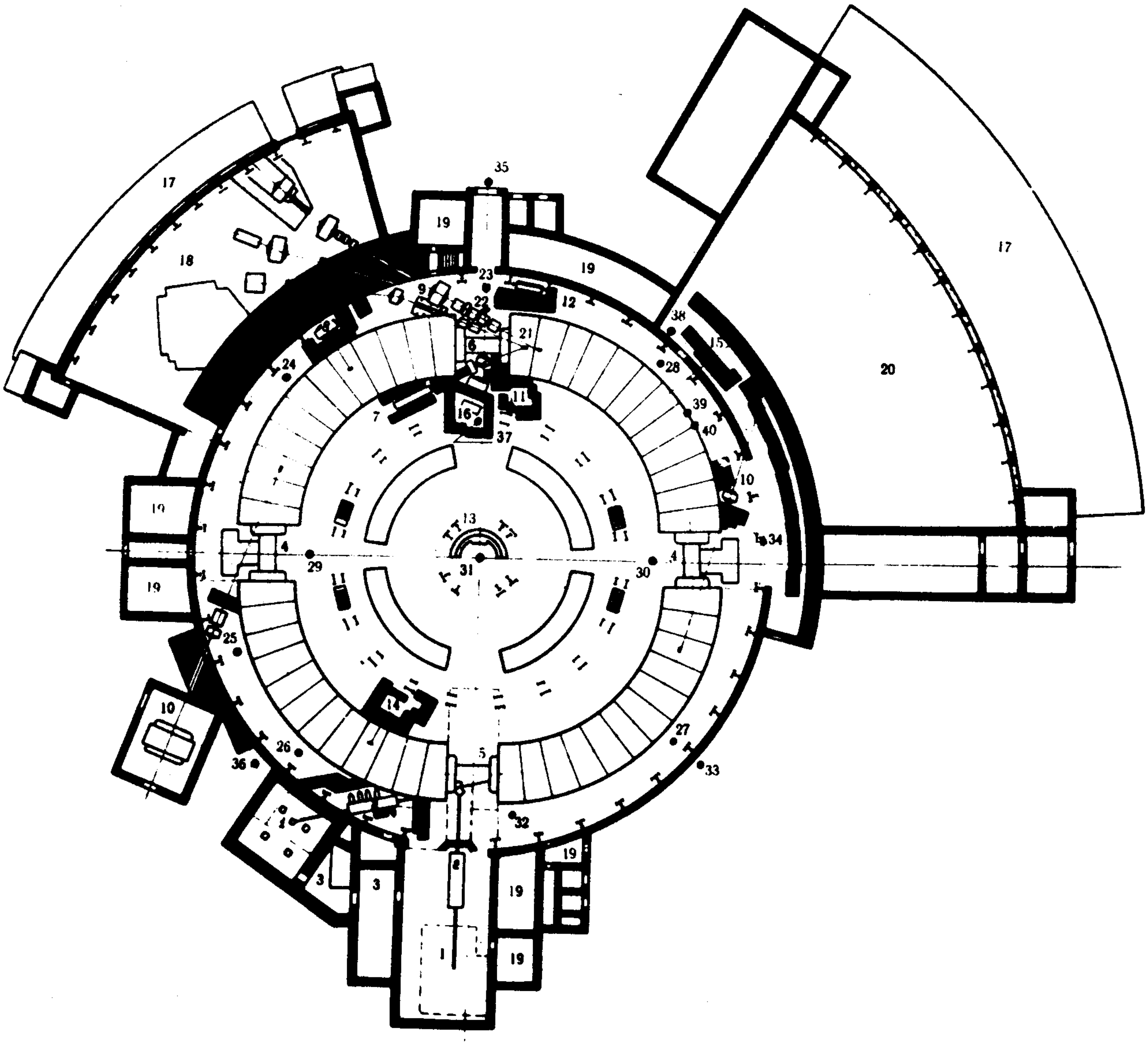

Fig. 1

SIS/R/12603

REFERENCES

1. V.I. Veksler et al., Atomnaya Energiya 4, 22 (1956).

2. A.N. Komaravskij, "Structural constitution of accelerators", Atomizdat, Moscow (1958).

3. B.I. Moyer, "Method of calculation of the shielding enclosure for the Berkeley Bevatron", Premier Colloque International sur la Protection auprès des Grands Accélérateurs., Presses Universitaires de France, 108 Bd. St. Germain, Paris (1962).

4. I.A. Geibel and I. Ranft, Nucl.Instr. and Methods, 32, 65-69 (1965).

5. L.S. Zolin, V.N. Lebedev and M.I. Salatskaya. JINR preprint 2251, Dubna (1965).

6. M.M. Komochkov and B.S. Sychev. Atomnaya Energiya 15, extract 4, 325 (1963).

7. S.J. Lindenbaum, Ann.Rev. of Nucl.Sci., 11, 213 (1961).

8. M.M. Komochkov. JINR preprint P-1349, Dubna (1963).

9. Sanitary rules for work with radioactive materials and ionizing radiation sources, No. 333-60, Gosatomizdat, M (1960).

10. R.N. Thomas, Berkeley California, private communication.

11. V.N. Lebedev, L.S. Zolin and M.I. Salatskaya. JINR preprint P-2177, Dubna (1965).

66/59/5
p/eht